A Hybrid Intelligent Approach for Metal-Loss Defect Depth Prediction in Oil and Gas Pipelines

Abduljalil Mohamed, Mohamed Salah Hamdi and Sofiène Tahar

Abstract The defect assessment process in oil and gas pipelines consists of three stages: defect detection, defect dimension (i.e., defect depth and length) prediction, and defect severity level determination. In this paper, we propose an intelligent system approach for defect prediction in oil and gas pipelines. The proposed technique is based on the *magnetic flux leakage* (MFL) technology widely used in pipeline monitoring systems. In the first stage, the MFL signals are analyzed using the Wavelet transform technique to detect any metal-loss defect in the targeted pipeline. In case of defect existence, an adaptive neuro-fuzzy inference system is utilized to predict the defect depth. Depth-related features are first extracted from the MFL signals, and then used to train the neural network to tune the parameters of the membership functions of the fuzzy inference system. To further improve the accuracy of the defect depth, predicted by the proposed model, highly-discriminant features are then selected by using the weight-based support vector machine (SVM). Experimental work shows that the proposed technique yields promising results, compared with those achieved by some service providers.

1 Introduction

It has been reported in [28] that the primary cause of approximately 30 % of defects in metallic long-distant pipelines, carrying crude oil and natural gas, is corrosion. To protect the surrounding environment from catastrophic consequences due to malfunctioning pipelines, an effective and efficient intelligent pipeline monitoringsystem

A. Mohamed (✉) · M.S. Hamdi
Information Systems Department, Ahmed Bin Mohammed Military College, Doha, Qatar
e-mail: ajamoham@abmmc.edu.qa

M.S. Hamdi
e-mail: mshamdi@abmmc.edu.qa

S. Tahar
Electrical and Computer Engineering Department, Concordia University,
Montreal, QC, Canada
e-mail: tahar@ece.concordia.ca

is required. Non-destructive evaluation (NDE)-based monitoring tools, such as magnetic sensors, are often employed to scan the pipelines [10, 29]. They are widely used, on a regular basis, to measure any *magnetic flux leakage* (MFL) that might be caused by defects such as corrosion, cracks, dents, etc. It has been observed that defect characteristics (for example defect depth) can be predicted by examining the shape and amplitude of the obtained MFL signals [2, 11, 27]. Thus, the majority of techniques reported in the literature rely heavily on the MFL signals. Other techniques that use other information sources such as ultrasonic waves and closed circuit television (CCTV) are also reported.

A reliability assessment of pipelines is a sequential process and consists mainly of three stages: defect detection and classification [5, 17, 18, 33, 35, 38], defect dimension prediction [22–24, 35], and defect severity assessment [9, 14, 34]. At the first stage, a defect may be reported by an inline inspection tool, mechanical damage accident, or visual examination. Then, the defect is associated to one of the possible defect types such as gouges on welds, dents, cracking, corrosion, etc. In the next stage, the dimensions (i.e., depth and length) of the identified defect are predicted. In the final stage, the defect severity level is determined. It is, based on the outcome of this stage that an immediate response, such as pressure reductions or pipe repair, may be deemed urgent. The defect depth is an essential parameter in determining the severity level of the detected defect. In [5], Artificial Neural Networks (ANNs) are first trained to distinguish defected MFL signals from normal MFL signals. In case of defect existence, ANNs are applied to classify the defect MFL signals into three defect types in the weld joint: external corrosion, internal corrosion, and lack of penetration. The proposed technique achieves a detection rate of 94.2 % and a classification accuracy of 92.2 %. The authors in [33] use image processing techniques to extract representative features from images of cracked pipes. To account for variations of values in these obtained features, a neuro-fuzzy inference system is trained such that the parameters of membership functions are tuned accordingly. A Radial Basis Function Neural Network (RBFNN) is trained to identify corrosion types in pipelines in [38], where artificial corrosion types are deliberately introduced on the pipeline, and the MFL data are then collected. The proposed Immune RBFNN (IRBFNN) was able to correctly locate the corrosion and determine its size. In [17], statistical and physical features are extracted from MFL signals and fed into a multi-layer perceptron neural network to identify defected signals. The identified defected signal is presented to a wavelet basis function neural network to generate a three-dimensional signal profile displayed on a virtual reality environment. In [18] a Support Vector Machine (SVM) is used to reconstruct shape features of three different defect types and used for defect classification and sizing. In [35], the authors propose a wavelet neural network approach for defect detection and classification in oil pipelines using MFL signals. In [22–24], artificial neural networks and neuro-fuzzy systems are used to estimate defect depths. In [22], static, cascaded, and dynamic feedforward neural networks are used for defect depth estimation. In [23], a self-organizing neural network is used as a visualization technique to identify appropriate features that are fed into different network architectures. In [24], a weight-based support vector machine is used to select the most relevant features that are fed into a neuro-fuzzy inference system.

For reliability assessment of pipelines, a fuzzy-neural network system is proposed in [34]. Sensitive parameters, representing the actual conditions of defected pipelines, are extracted from MFL signals and used to train the hybrid intelligent system. The intelligent system is then used to estimate the probability of failure of the defected pipeline. The authors in [9] propose an artificial neural network approach for defect classification using some defect-related factors including metal-loss, age, operating pressure, pipeline diameter. In [14], to reduce the number of features used in the defect assessment stage, several techniques are utilized including support vector machine, regression, principal component analysis, and partial least squares.

The rest of the paper is organized as follows. In Sect. 2, we review the reliability assessment process in oil and gas pipelines. The proposed hybrid intelligent system for defect depth prediction is introduced in Sect. 3. In Sect. 4, the performance evaluation of the proposed approach is described. We conclude with final remarks in Sect. 5.

2 Reliability Assessment of Oil and Gas Pipelines

The main components of the reliability assessment process of pipelines are shown in Fig. 1. After detecting the presence of a pipeline defect, the pipeline reliability assessment system estimates the size of the defect (i.e. its length and depth), and based on that, it predicts the severity of the defect and takes a measureable action to rectify the situation. In the following we briefly describe each component.

2.1 Data Processing

Nondestructive evaluation (NDE) tools are often used to scan pipelines for potential defects. One of these NDE tools are magnetic sensors that are attached to autonomous devices sent periodically into the pipeline under inspection. The purpose of magnetic sensors is to measure MFL signals [20], every 3 mm along the pipeline length. A sample of a MFL signal is shown in Fig. 2. The amount of MFL data is huge, thus feature extraction methods are needed to reduce data dimensionality. However, using
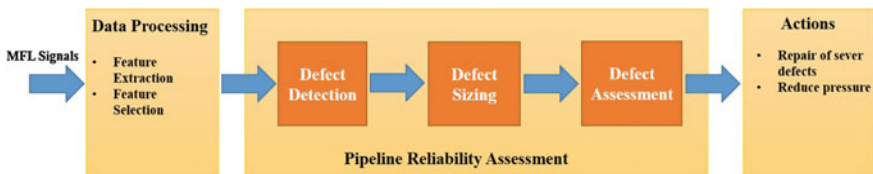
Fig. 1 Reliability assessment of pipelines
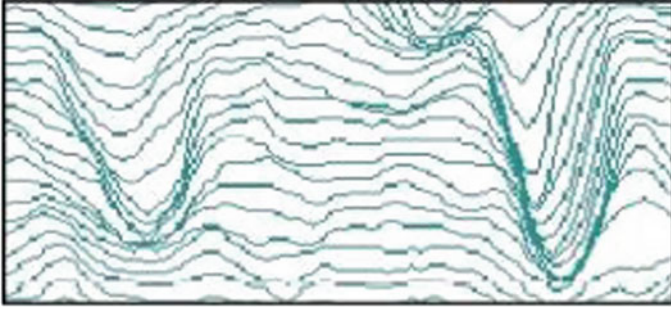
Fig. 2 A sample of a MFL signal

all the extracted features may not actually lead to a better reliability assessment performance. Thus, the most relevant features are selected and fed into the detection and sizing units.

2.2 Defect Detection

Once the processed MFL signals are received, techniques such as wavelets can be used to detect and locate defects on the pipe surface [11]. Wavelet techniques are powerful mathematical tools [8, 19, 21]. They were used in many applications such as data compression [4], data analysis and classification [36], and de-noising [26, 27, 32]. The wavelet technique can also be used to locate defects on the targeted pipeline as follows. The MFL signal contains three components and each of these components consists of a sum of curves, and these are a translated and dilated version of a reference pattern. Suppose the mother wavelet $\psi(x)$ refer to the reference pattern, and $\langle \psi_{j,k}(x) \rangle$ is the wavelet basis. Thus, the MFL signal $B(x)$ can be represented as:

$$B(x) = \sum_{j,k} c_{j,k} \psi_{j,k}(x) \tag{1}$$

When the wavelet transform of the MFL signal ($B(x)$) is computed with respect to the basis $\langle \psi_{j,k}(x) \rangle$, the set of non-zero coefficients $c_{j,k}$ indicate the locations of metal-loss defects on the surface of the pipeline. Moreover, the set of dilation factors of the reference pattern is determined, which yields the widths of the defects.

2.3 Defect Sizing

Defect sizing (in particular, determination of the defect depth) is an essential component of the reliability assessment system as, based on its outcome, the severity of the detected defect can be determined. However, the relationship between the measured MFL signals and the corresponding defect depth is not well-understood. Therefore, in the absence of feasible analytical models, hybrid intelligent tools such as Adaptive Neuro-Fuzzy Inference systems (ANFIS) become indispensable and can be used to learn this relationship [22–24, 35]. In this paper, after extracting and selecting meaningful features, an ANFIS model is trained using a hybrid learning algorithm that comprises least squares and the backpropagation gradient descent method [13].

2.4 Defect Assessment

Upon calculating the dimensions of the defect, its severity level can be determined by using the industry standard [1]. Basic equations for assessing defects can be used to construct defect acceptance curves as shown in Fig. 3 [7]. The first curve calculates the failure stress of defects in the pipeline at the maximum operating pressure (MAOP), and the other curve shows the sizes of defects that would fail the hydro pressure test [7].

2.5 Actions

The plot in Fig. 3 can be used to prioritize the repair of the defects. For example, two defects are predicted to fail at the MAOP. For these defects, an immediate repair is needed. Defects that have failure stresses lower than the hydro pressure curve are acceptable. Any defect between the assessing curves needs to be reassessed using advanced measuring tools.

3 A Hybrid Intelligent System for Defect Depth Estimation

The combination of neural networks and fuzzy inference systems has been successfully used in different application areas such as water quality management [31], queue management [25], energy [37], transportation [15]; and business and manufacturing [6, 12, 16, 30]. In this section, the applicability of ANFIS models in estimating metal-loss defect depth is demonstrated. The general architecture of the proposed approach is shown in Fig. 4.
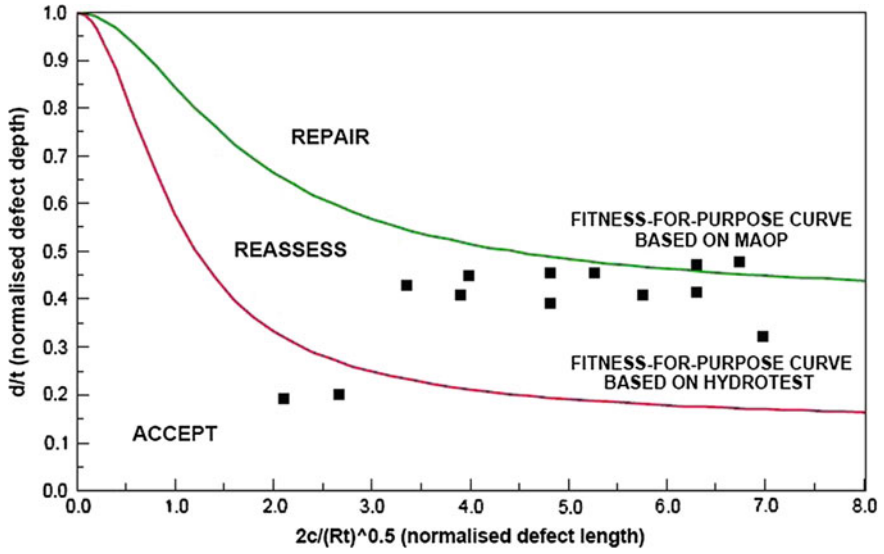
Fig. 3 Curves of defect assessment (Reproduced from [7])
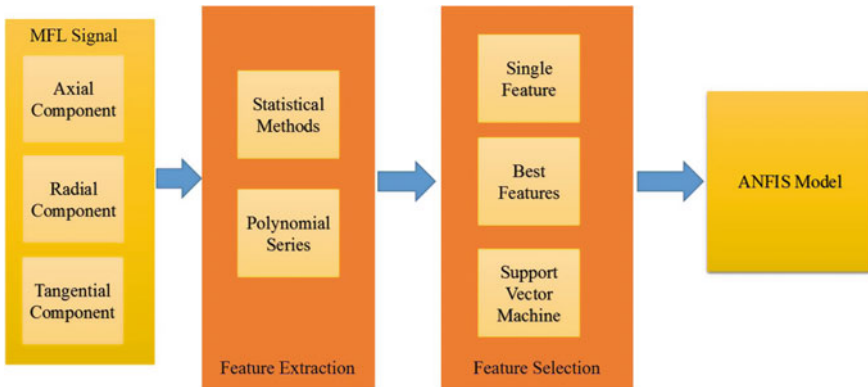
Fig. 4 The structure diagram of the proposed approach

The proposed approach consists of three stages, namely: feature extraction, feature selection, and the ANFIS model. The three components are described in the following subsections.
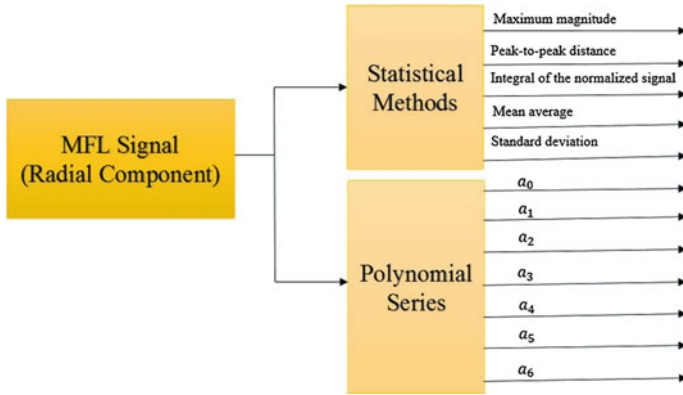
Fig. 5 Features extracted for the radial component of the MFL signal

3.1 Feature Extraction

The main purpose of feature extraction is to reduce the MFL data dimensionality. As shown in Fig. 4, the MFL signal is represented by the axial, radial and tangential components. For each component, statistical and polynomial series are applied as feature extraction methods. The features extracted from the radial component of the MFL signal are shown in Fig. 5. Statistical features are self-explanatory. Polynomial series of the form $a_n X^n + \cdots + a_1 X + a_0$ can approximate MFL signals. Polynomials of degrees 3, 6, and 6 have been found to provide the best approximation for axial, radial, and tangential components, respectively. Thus, the input features consist of the polynomial coefficients, $a_n, \ldots, a_0$ along with the five statistical features. Thus, in total we have 33 features, which will be referred to by F1, F2,…, F33.

3.2 Feature Selection

It is a known fact that different features might exhibit different discrimination capabilities. Most often, incorporating all obtained features in the training process may not lead to a high depth estimation accuracy. In fact, including some features may have a negative impact. Therefore, it is a common practice to identify the important features that are appropriate to the ANFSI model. Thus, the next step is to examine the suitability of each feature for the defect depth prediction task. The best features that yield the best depth estimation accuracy are then identified and used as an input feature pattern for the ANFIS model. Moreover, a support vector machine-based weight correlation method is used to assign weights for the obtained features. Features with the highest weights are selected to train a new ANFIS model. Different sets of features, having 16 to 29 features each, have been evaluated.
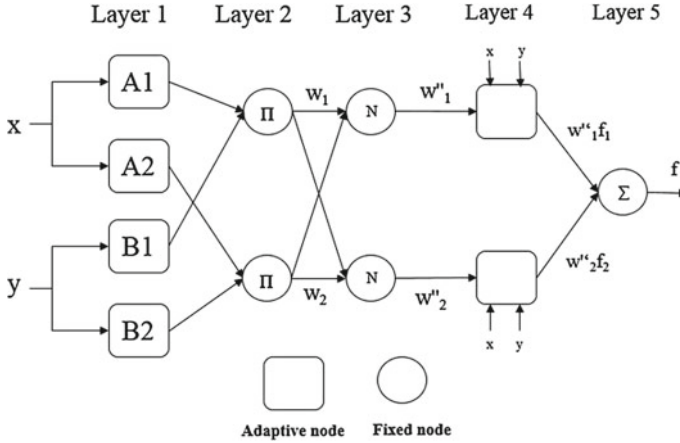
Fig. 6 The architecture of ANFIS

3.3 The ANFIS Model

ANIFIS, as introduced by [13], is a hybrid neuro-fuzzy system, where the fuzzy
IF-THEN rules and membership function parameters can be learned from training
data, instead of being obtained from an expert [3, 6, 12, 16, 25, 30, 31, 37]. Whether
the domain knowledge is available or not, the adaptive property of some of its nodes
allows the network to generate the fuzzy rules that approximate a desired set of
input-output pairs. In the following, we briefly introduce the ANFIS architecture as
proposed in [13]. The structure of the ANFIS model is basically a feedforward multi-
layer network. The nodes in each layer are characterized by their specific function,
and their outputs serve as inputs to the succeeding nodes. Only the parameters of
the adaptive nodes (i.e., square nodes in Fig. 6) are adjustable during the training
session. Parameters of the other nodes (i.e., circle nodes in Fig. 6) are fixed.

Suppose there are two inputs x, y, and one output f. Let us also assume that
the fuzzy rule in the fuzzy inference system is depicted by one degree of Sugeno's
function [13]. Thus, two fuzzy *if-then* rules will be contained in the rule base as
follows:

Rule 1: if x is A_1 and y is B_1 then $f = p_1 x + q_1 y + r_1$.
Rule 2: if x is A_2 and y is B_2 then $f = p_2 x + q_2 y + r_2$.
where p_i, q_i, r_i are adaptable parameters.
The node functions in each layer are described in the sequel.
Layer 1: Each node in this layer is an adaptive node and is given as follows:

$$o_i^1 = \mu_{Ai}(x), \quad i = 1, 2 \tag{2}$$

$$o_i^1 = \mu_{Bi-2}(y), \quad i = 3, 4 \tag{3}$$

where x and y are inputs to the layer nodes, and A_i, B_{i-2} are linguistic variables. The maximum and minimum of the bell-shaped membership function are 1 and 0, respectively. The membership function has the following form:

$$\mu_{Ai}(x) = \frac{1}{1 + \{(\frac{x-c_i}{a_i})^2\}^{bi}} \tag{4}$$

where the set $\{a_i, b_i, c_i\}$ represents the premise parameters of the membership function. The bell-shaped function changes according to the change of values in these parameters.

Layer 2: Each node in this layer is a fixed node. Its output is the product of the two input signals as follows:

$$o_i^2 = w_i = \mu_{Ai}(x)\mu_{Bi}(y), \quad i = 1, 2 \tag{5}$$

where w_i refers to the firing strength of a rule.

Layer 3: Each node in this layer is a fixed node. Its function is to normalize the firing strength as follows:

$$o_i^3 = w_i'' = \frac{w_i}{w_1 + w_2}, \quad i = 1, 2 \tag{6}$$

Layer 4: Each node in this layer is adaptive and adjusted as follows:

$$o_i^4 = w_i'' f_i = w_i''(p_i x + q_i y + r_i), \quad i = 1, 2 \tag{7}$$

where w_i'' is the output of layer 3 and $\{p_i + q_i + r_i\}$ is the consequent parameter set.

Layer 5: Each node in this layer is fixed and computes its output as follows:

$$o_i^5 = \sum_{i=1}^{2} w_i'' f_i = \frac{(\sum_{i=1}^{2} w_i f_i)}{w_1 + w_2} \tag{8}$$

The output of layer 5 sums the outputs of nodes in layer 4 to be the output of the whole network. If the parameters of the premise part are fixed, the output of the whole network will be the linear combination of the consequent parameters, i.e.,

$$f = \frac{w_1}{w_1 + w_2} f_1 + \frac{w_2}{w_1 + w_2} f_2 \tag{9}$$

The adopted training technique is hybrid, in which, the network node outputs go forward till layer 4, and the resulting parameters are identified by the least square method. The error signal, however, goes backward till layer 1, and the premise parameters are updated according to the descent gradient method. It has been shown

in the literature that the hybrid-learning technique can obtain the optimal premise
and consequent parameters in the learning process [13].

3.4 Learning Algorithm for ANFIS

To map the input/output data set, the adaptable parameters $\{a_i + b_i + c_i\}$ and $\{p_i +
q_i + r_i\}$ in the ANFIS structure are adjusted in the learning process. When the premise
parameters a_i, b_i and c_i of the membership function are fixed, the ANFIS yields the
following output as shown in (9). Substituting (6) into (9), we obtain the following:

$$f = w_1'' f_1 + w_2'' f_2 \tag{10}$$

Substituting the fuzzy *if-then* rules in (10) yields:

$$f = w_1''(p_1 x + q_1 y + r_1) + w_2''(p_2 x + q_2 y + r_2) \tag{11}$$

or:

$$f = (w_1'' x)p_1 + (w_1'' y)q_1 + (w_1'')r_1 + (w_2'' x)p_2 + (w_2'' y)q_2 + (w_2'')r_2 \tag{12}$$

Equation (12) is a linear combination of the adjustable parameters. The optimal
values of $\{a_i, b_i, c_i\}$ and $\{p_i, q_i, r_i\}$ can be obtained by using the least squared method.
If the premise parameters are fixed, the hybrid learning algorithm can effectively
search for the optimal ANFIS parameters.

4 Experimental Results

To evaluate the effectiveness of the proposed technique, in terms of defect depth
estimation accuracy, extensive experimental work has been carried out. The obtained
accuracies are evaluated based on different levels of error-tolerance including: ± 1,
± 5, ± 10, ± 15, ± 20, ± 25, ± 30, ± 35, and $\pm 40\%$. The impact of using selected
features, while utilizing different number and type of membership functions for
the adaptive nodes in the ANFIS model is studied. The results are reported in the
following subsections.

4.1 Types of Membership Functions for the Adaptive Nodes

The shape of the selected membership function (MF) defines how each point in the
universe of discourse of the corresponding feature is mapped into a membership

value between 0 and 1 (the membership value indicates the degree to which the relevant input feature belongs to a certain metal-loss defect depth). The parameters that control the shape of the membership function are tuned in the adaptive nodes, during the training session. The number of parameters needed depends on the type of the membership function used in the adaptive node. Three types of membership functions namely Gaussian, Trapezoidal, and Triangle for the feature F1 are shown in Fig. 7.

It can be seen from Fig. 7 that the smoothness of transition from one fuzzy set to another varies, depending on the function type used in the adaptive node.

4.2 Training, Testing, and Validation Data

During the training session, four of the obtained features, namely F3, F6, F8, and F13, were not acceptable by the Matlab ANFIS model. Their sigma values were close to zero so they were discarded. Thus, only 29 features of the 33 above mentioned features were considered. The 1357 data samples, used for developing and testing the ANFIS model, were divided as follows: 70 % for training, 15 % for testing, and 15 % for validation (checking). The training data set consists of 949 rows and 30 columns. The rows represent the training samples, and the first 29 columns represent the extracted features of each sample and the last column represents the target (defect depth). The format of the testing and validation data sets is similar to that of the training data set, however, each consists of 204 rows (samples). We have used 100 epochs to train the ANFIS model.

A hybrid learning approach was adopted, in which the membership function parameters of the single-out Sugeno type fuzzy inference system were identified. The hybrid learning approach converges much faster than the original backpropagation method. In the forward pass, the node outputs go forward until layer 4 and the consequent parameters are identified with the least square method. In the backward pass, the error rates propagate backwards and the premise parameters are updated by gradient decent.

4.3 Evaluation of the Feature Prediction Power

In this section, the performance of each feature, in terms of its defect depth prediction accuracy, is examined. Due to limited space, only the features that yield the best prediction accuracy are reported. As shown in Table 1, seven features present the best estimation accuracy among all features, namely F1, F4, F9, F10, F11, F14, and F32. As expected, for the lower levels of error tolerance (particularly: ± 10, ± 15, and $\pm 20 \%$), none of the features yielded an acceptable prediction accuracy.
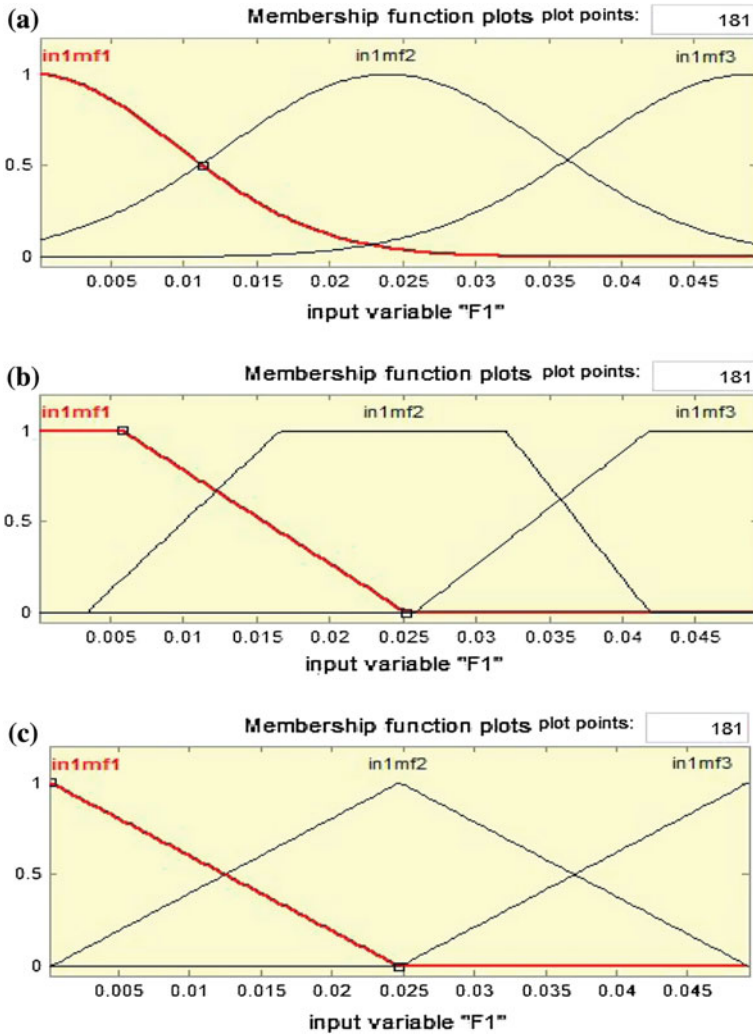
Fig. 7 Membership functions of the feature F1 **a** Gaussian, **b** trapezoidal, and **c** triangle

4.4 Using the Best Features

To improve the defect depth prediction accuracy of the ANFIS model, the features that yield the best prediction accuracy are used to train the ANFIS model. For 100 epochs, the training performance error of the ANFIS model is equal to 0.1482. The defect depth prediction accuracy of this model is clearly improved as shown in Table 2. For error-tolerance levels at ±10, ±15, and ±20 %, the model gives prediction accuracy at 62, 74, and 87 %, respectively.

Table 1 Defect depth prediction accuracy using the features F1, F4, F9, F10, F11, F14, and F32

Error-tolerance (%)	Input parameters						
	F1	F4	F9	F10	F11	F14	F32
±1	0.0196	0.0147	0.0294	0.0490	0.0196	0.0147	0.0392
±5	0.1176	0.1275	0.1618	0.1176	0.1373	0.1618	0.1275
±10	0.2892	0.2990	0.3627	0.2304	0.3235	0.2941	0.2941
±15	0.4510	0.4755	0.5637	0.4118	0.4902	0.5000	0.4608
±20	0.6275	0.6471	0.7549	0.5686	0.6667	0.6618	0.5882
±25	0.8137	0.8039	0.9265	0.6912	0.8137	0.8578	0.7010
±30	0.8775	0.8971	0.9461	0.7990	0.9020	0.9167	0.8480
±35	0.9265	0.9314	0.9510	0.9020	0.9412	0.9363	0.8922
±40	0.9461	0.9510	0.9559	0.9314	0.9559	0.9461	0.9265

Table 2 Defect depth prediction accuracy of the ANFIS model using the best features

Error-tolerance (%)	Input features (F1 F4 F9 F10 F11 F14 F32)
±1	0.0637
±5	0.3529
±10	0.6127
±15	0.7402
±20	0.8725
±25	0.9314
±30	0.9510
±35	0.9755
±40	0.9853

4.5 Support Vector Machine-Based Feature Selection

Another method for evaluating the prediction power of the obtained features is by assigning a weight for each feature, based on the support vector machine weight-correlation technique. Features with the highest weights are selected to train the ANFIS model. After examining different sets of selected features, the first 22 features have yielded the best prediction accuracy as demonstrated in Table 3.

As shown in Table 3, for error-tolerance levels at ±10, ±15, and ±20 %, the model gives a prediction accuracy at 62, 80, and 87 %, respectively. It is slightly improved over the best features, reported in Table 2. For the error-tolerance level at ±10 %, the prediction accuracy improved 1 %, and for ±15 %, improved 6 %. However, for the ±20 % error-tolerance level, it remained the same as that of the best features. Only, using all the 29 features can give comparable results (shown in the last column of Table 3).

Table 3 Defect depth prediction accuracy of the ANFIS model using 22 features and all features

Error-tolerance (%)	22 Input features	All features
±1	0.0637	0.0588
±5	0.3529	0.3627
±10	0.6225	0.6324
±15	0.8039	0.7990
±20	0.8775	0.8529
±25	0.9118	0.8971
±30	0.9559	0.9314
±35	0.9706	0.9510
±40	0.9804	0.9608

4.6 Using Different Membership Function Types

In this section, we examine the impact of using three different membership function types on the model performance. In the model adaptive nodes, to each of the seven best features (i.e., F1, F4, F9, F10, F11, F14, and F32), we assigned Gaussian, trapezoidal, and triangle membership functions. The shapes of these functions are shown in Fig. 7. The number of membership functions is set at 2 or 3, for each type. The outputs of the ANFIS model for the training, testing and validation data (for Gaussian membership function) are shown in Fig. 8. The x-axis represents the indices of the training data elements, whereas the y-axis represents the defect depths of the corresponding data elements. The 949 training data samples, representing the true defect depths, are plotted in blue (Fig. 8a). While the model out puts, representing the same defect depths estimated by the model, are plotted in red (Fig. 8a). Clearly, the model outputs (estimated defect depths) are satisfactory as they lie on or close to the true defect depths. Figure 8b, c show the model outputs (plotted in red) against the 204-element testing data (plotted in blue) and 204-element validation (checking) data (plotted in blue), respectively. The defect depth prediction accuracy, obtained by the ANFIS model for the three types of membership functions, is shown in Table 4, where the best accuracies are highlighted in red.

The model shows improvement for the error-tolerance levels ±1, ±5, and ±10 % as it yield 11, 48, and 71 %, respectively, compared to 6, 35, and 62 % produced by the ANFIS model using the 22 features. For the rest of the error-tolerance levels, it yields accuracies comparable to those produced by the ANFIS model using the 22 features. The best training error is calculated at 0.106, obtained by the ANFIS model using three triangle membership functions.
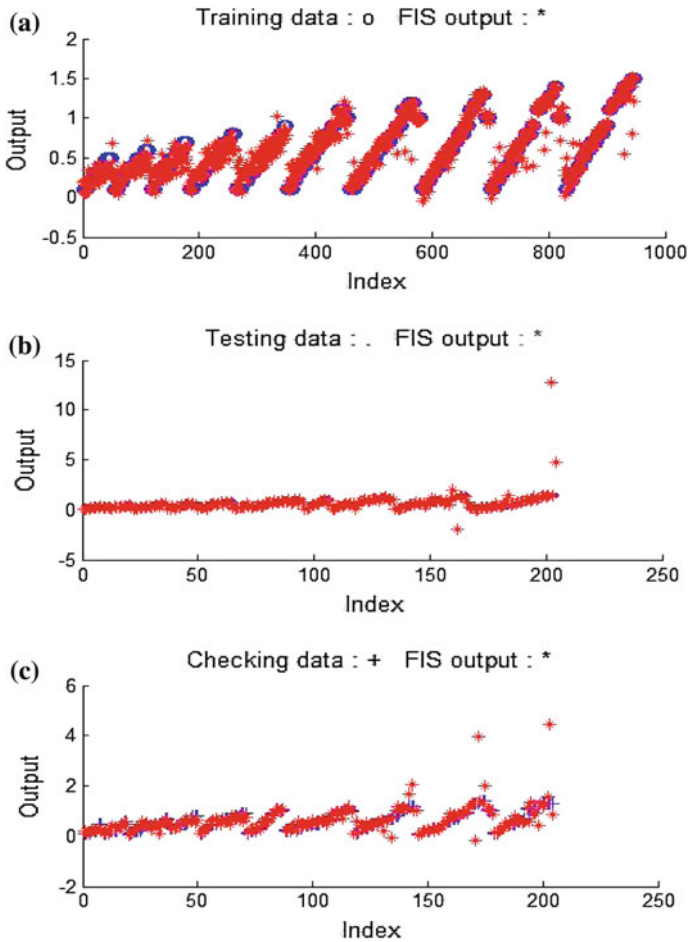
Fig. 8 The outputs of the ANFIS model (*red*) using the Gaussian membership function at the adaptive node: training data (**a**), testing data (**b**), and validation data (**c**), shown in *blue*

5 Conclusions

In order to assess the reliability of a functioning oil and gas pipeline, the depth of a detected defect should be first determined. Based on which, appropriate maintenance actions are carried out. In this work, a hybrid intelligent approach for metal-loss defect depth prediction in oil and gas pipelines is proposed. The proposed approach utilizes MFL data acquired by magnetic sensors scanning the metallic pipelines. To reduce the MFL data, feature extraction methods are applied. The extracted features are fed into an adaptive neuro-fuzzy inference system (ANFIS), individually, to examine their depth prediction capabilities. The most effective features are then

Table 4 Defect depth prediction accuracy of the ANFIS model using three different numbers and types of membership functions

No of functions	Function type	Learning algorithm	Training error	Depth prediction accuracy		
				±1%	±5%	±10%
2	Gaussian	Hybrid	0.122	0.0588	0.3971	0.6324
2	Triangle	Hybrid	0.127	0.0539	0.3480	0.6176
2	Trapezoidal	Hybrid	0.131	0.0735	0.3775	0.6422
3	Gaussian	Hybrid	0.108	0.1029	0.4412	0.6814
3	Triangle	Hybrid	0.106	0.1176	0.4853	0.7108
3	Trapezoidal	Hybrid	0.114	0.0588	0.3382	0.6324
No of functions	Function type	Learning algorithm	Training error	Depth prediction accuracy		
				±15%	±20%	±25%
2	Gaussian	Hybrid	0.122	0.7892	0.8873	0.9167
2	Triangle	Hybrid	0.127	0.7794	0.8578	0.8971
2	Trapezoidal	Hybrid	0.131	0.7647	0.8627	0.9069
3	Gaussian	Hybrid	0.108	0.7941	0.8480	0.8676
3	Triangle	Hybrid	0.106	0.7843	0.8235	0.8627
3	Trapezoidal	Hybrid	0.114	0.7794	0.8382	0.8676
No of functions	Function type	Learning algorithm	Training error	Depth prediction accuracy		
				±30%	±35%	±40%
2	Gaussian	Hybrid	0.122	0.9461	0.9657	0.9657
2	Triangle	Hybrid	0.127	0.9314	0.9461	0.9608
2	Trapezoidal	Hybrid	0.131	0.9363	0.9510	0.9510
3	Gaussian	Hybrid	0.108	0.9020	0.9216	0.9363
3	Triangle	Hybrid	0.106	0.8775	0.8922	0.9020
3	Trapezoidal	Hybrid	0.114	0.8873	0.9167	0.9216

identified and used to retrain the ANFIS model. Utilizing different types and numbers of membership functions, the proposed ANFIS model is tested for different levels of error-tolerance. At the levels of ±10, ±15, and ±20%, the best defect depth prediction obtained by the new approach are 71, 79, and 88%, using triangle, triangle, and Gaussian membership functions, respectively. In future work, sophisticated feature extraction methods will be investigated to enhance the model performance. Moreover, the uncertainty properties, inherently pertaining to the magnetic sensors, will also be addressed.

References

1. American Society of Mechanical Engineers: ASME B31G Manual for Determining Remaining Strength of Corroded Pipelines (1991)
2. Amineh, R., et al.: A space mapping methodology for defect characterization from magnetic flux leakage measurement. IEEE Trans. Magn. **44**(8), 2058–2065 (2008)
3. Azamathulla, H., Ab Ghani, A., Yen Fei, S.: ANFIS-based approach for predicting sediment transport in clean sewer. Appl. Soft Comput. **12**(3), 1227–1230 (2012)
4. Bradley, J., Bradley, C., Brislawn, C., Hopper, T.: FBI wavelet/scalar quantization standard for gray-scale fingerprint image compression. SPIE Proc., Visual Inf. Process. II **1961**, 293–304 (1993)
5. Carvalho, A., et al.: MFL signals and artificial neural network applied to detection and classification of pipe weld defects. NDT Int. **39**(8), 661–667 (2006)
6. Chen, M.: A hybrid ANFIS model for business failure prediction utilizing particle swarm optimization and subtractive clustering. Inf. Sci. **220**, 180–195 (2013)
7. Cosham, A., Kirkwood, M.: Best practice in pipeline defect assessment. Paper IPC00-0205, International Pipeline Conference (2000)
8. Daubechies, I.: Ten Lectures on Wavelets. SIAM: Society for Industrial and Applied Mathematics, Philadelphia (1992)
9. El-Abbasy, M., et al.: Artificial neural network models for predicting condition of offshore oil and gas pipelines. Autom. Constr. **45**, 50–65 (2014)
10. Gloria, N., et al.: Development of a magnetic sensor for detection and sizing of internal pipeline corrosion defects. NDT E Int. **42**(8), 669–677 (2009)
11. Hwang, K., et al.: Characterization of gas pipeline inspection signals using wavelet basis function neural networks. NDT E Int. **33**(8), 531–545 (2000)
12. Iphar, M.: ANN and ANFIS performance prediction models for hydraulic impact hammers. Tunn. Undergr. Space Technol. **27**(1), 23–29 (2012)
13. Jang, J.: ANFIS: adaptive-network-based fuzzy inference system. IEEE Trans. Syst., MAN, Cybern. **23**, 665–685 (1993)
14. Khodayari-Rostamabad, A., et al.: Machine learning techniques for the analysis of magnetic flux leakage images in pipeline inspection. IEEE Trans. Magn. **45**(8), 3073–3084 (2009)
15. Khodayari, A., et al.: ANFIS based modeling and prediction car following behavior in real traffic flow based on instantaneous reaction delay. In: IEEE Intelligent Transportation Systems Conference, pp. 599–604 (2012)
16. Kulaksiz, A.: ANFIS-based estimation of PV module equivalent parameters: application to a stand-alone PV system with MPPT controller. Turk. J. Electr. Eng. Comput. Sci. **21**(2), 2127–2140 (2013)
17. Lee, J., et al.: Hierarchical rule based classification of MFL signals obtained from natural gas pipeline inspection. In: International Joint Conference on Neural Networks, vol. 5 (2000)
18. Lijian, Y., et al.: Oil-gas pipeline magnetic flux leakage testing defect reconstruction based on support vector machine. In: Second International Conference on Intelligent Computation Technology and Automation, vol. 2 (2009)
19. Mallat, S.: A Wavelet Tour of Signal Processing. Academic, New York (2008)
20. Mandal, K., Atherton, D.: A study of magnetic flux-leakage signals. J. Phys. D: Appl. Phys. **31**(22), 3211 (1998)
21. Misiti, M., Misiti, Y., Oppenheim, G., Poggi, J.: Wavelets and Their Applications. Wiley-ISTE, New York (2007)
22. Mohamed, A., Hamdi, M.S., Tahar, S.: A machine learning approach for big data in oil and gas pipelines. In: 3rd International Conference on Future Internet of Things and Cloud (2015)
23. Mohamed, A., Hamdi, M.S., Tahar, S.: Self-organizing map-based feature visualization and selection for defect depth estimation in oil and gas pipelines. In: 19th International Conference on Information Visualization (2015)

24. Mohamed, A., Hamdi, M.S., Tahar, S.: An adaptive neuro-fuzzy inference system-based approach for oil and gas pipeline defect depth estimation. In: SAI Intelligent Systems Conference (2015)
25. Mucsi, K., Ata, K., Mojtaba, A.: An adaptive neuro-fuzzy inference system for estimating the number of vehicles for queue management at signalized intersections. Transp. Res. Part C: Emerg. Technol. **19**(6), 1033–1047 (2011)
26. Muhammad, A., Udpa, S.: Advanced signal processing of magnetic flux leakage data obtained from seamless gas pipeline. NDT E Int. **35**(7), 449–457 (2002)
27. Mukhopadhyay, S., Srivastave, G.: Characterization of metal-loss defects from magnetic signals with discrete wavelet transform. NDT Int. **33**(1), 57–65 (2000)
28. Nicholson, P.: Combined CIPS and DCVG survey for more accurate ECDS data. J. World Pipelines **7**, 1–7 (2007)
29. Park, G., Park, E.: Improvement of the sensor system in magnetic flux leakage-type non-destructive testing. IEEE Trans. Magn. **38**(2), 1277–1280 (2002)
30. Petković, D., et al.: Adaptive neuro-fuzzy estimation of conductive silicone rubber mechanical properties. Expert Syst. Appl. **39**(10), 9477–9482 (2012)
31. Roohollah, N., Safavi, S., Shahrokni, S.: A reduced-order adaptive neuro-fuzzy inference system model as a software sensor for rapid estimation of five-day biochemical oxygen demand. J. Hydrol. **495**, 175–185 (2013)
32. Shou-peng, S., Pei-wen, Q.: Wavelet based noise suppression technique and its application to ultrasonic flaw detection. Ultrasonics **44**(2), 188–193 (2006)
33. Sinha, S., Karray, F.: Classification of underground pipe scanned images using feature extraction and neuro-fuzzy algorithm. IEEE Trans. Neural Netw. **13**(2), 393–401 (2002)
34. Sinha, S., Pandey, M.: Probabilistic neural network for reliability assessment of oil and gas pipelines. Comput.-Aided Civil Infrastruct. Eng. **17**(5), 320–329 (2002)
35. Tikaria, M., Nema, S.: Wavelet neural network based intelligent system for oil pipeline defect characterization. In: 3rd International Conference on Emerging Trends in Engineering and Technology (ICETET) (2010)
36. Unser, M., Aldroubi, A.: A review of wavelets in biomedical applications. Proc. IEEE **84**(4), 626–638 (1996)
37. Zadeh, A., et al.: An emotional learning-neuro-fuzzy inference approach for optimum training and forecasting of gas consumption estimation models with cognitive data. Technol. Forecast. Soc. Change **91**, 47–63 (2015)
38. Zhongli, M., Liu, H.: Pipeline defect detection and sizing based on MFL data using immune RBF neural networks. In: IEEE Congress on Evolutionary Computation pp. 3399–3403 (2007)